Journal of Integrative Agriculture 2026, 25(1): 352–365

Available online at ScienceDirect

Journal of Integrative Agriculture

RESEARCH ARTICLE

Mechanical stress induces molecular changes in oolong tea: Insights from multi-omics analysis

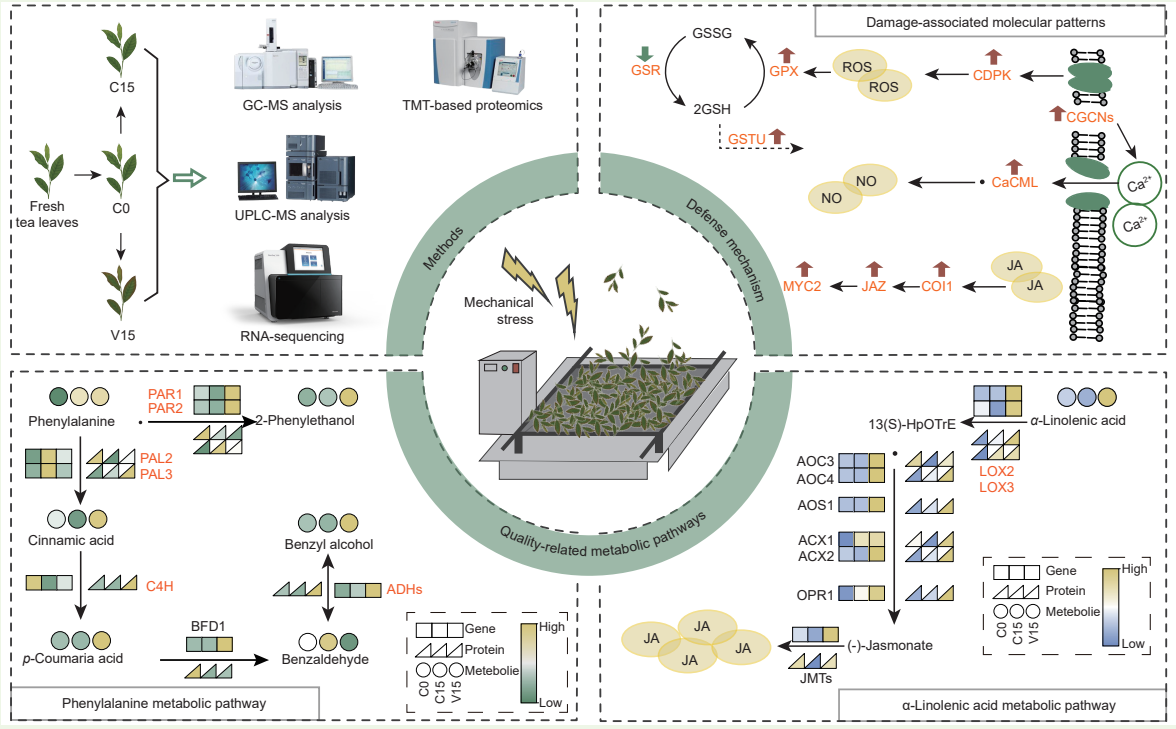
Zhilong Hao[1, 2*#], Yuping Zhang[1, 3*], Weiyi Kong[1, 3], Jiao Feng[1, 3], Yucheng Zheng[4], Hongzheng Lin[5], Xiaomin Yu[1], Yun Sun[1, 2], Xiangxiang Huang[1, 2], Wei Wang[1, 2], Yang Wu[1, 2#], Xinyi Jin[1, 2#]

[1] *College of Horticulture, Fujian Agriculture and Forestry University, Fuzhou 350002, China*
[2] *Key Laboratory of Tea Science in Universities of Fujian Province, Fuzhou 350002, China*
[3] *Tea Industry Branch of 6.18 Collaborative Innovation Institute in Fujian Province, Fuzhou 350002, China*
[4] *College of Tea and Food Sciences/Tea Engineering Research Center of Fujian Higher Education/Tea Science Research Institute, Wuyi University, Wuyishan 354300, China*
[5] *Fujian Vocational College of Agriculture, Fuzhou 350303, China*

Highlights

- Integrated multi-omics (metabolomics, transcriptomics, proteomics) elucidates tea leaf responses to mechanical stress.
- Mechanical stress-activated DAMPs ignite the Ca^{2+}-JA-GSH signaling cascade, orchestrating downstream aroma biosynthesis.
- Mechanical stress induces *LOX*/*PAR* genes and their encoded proteins in *α*-linolenic/Phe metabolism, boosting accumulation of 2-phenylethanol and jasmine lactone.

Graphical abstract



Received 14 May 2025; Received in revised form 21 July 2025; Accepted 9 August 2025; Available online 12 September 2025
[#]Correspondence Zhilong Hao, E-mail: haozhilong@126.com; Yang Wu, E-mail: wy_forward@fafu.edu.cn; Xinyi Jin, E-mail: jxy427@tom.com
[*]These authors contributed equally to this sthdy.

© 2026 CAAS. Publishing services by Elsevier B.V. on behalf of KeAi Communications Co. Ltd. This is an open access article under the CC BY-NC-ND license (http://creativecommons.org/licenses/by-nc-nd/4.0/). Peer review under responsibility of Editorial Board of *Journal of Integrative Agriculture*.
doi: 10.1016/j.jia.2025.09.014

Abstract

Understanding the molecular responses of tea leaves to mechanical stress is crucial for elucidating the mechanisms of post-harvest quality formation during oolong tea processing. This study employed an integrated multi-omics strategy to characterize the changes and interactions among metabolomic (MB), transcriptomic (TX), and proteomic (PT) profiles in mechanically stressed tea leaves. Mechanical stress initially activated damage-associated molecular patterns (DAMPs), including Ca^{2+} signaling, jasmonic acid signaling, and glutathione metabolism pathways. These processes subsequently induced quality-related metabolic pathways (QRMPs), particularly *α*-linolenic acid and phenylalanine metabolism. Up-regulated expression of *LOX*, *ADH1*, and *PAR* genes, together with the increased abundance of their encoded proteins, respectively promoted the accumulation of jasmine lactone, benzyl alcohol, and 2-phenylethanol. These findings indicate that mechanical stress influences the metabolite biosynthesis in tea leaves through coordinated molecular responses. This study provides new insights into the molecular mechanisms underlying tea leaf responses to mechanical stress and a foundation for future investigations into how early molecular events may contribute to post-harvest metabolic changes during oolong tea processing.

Keywords: oolong tea, multi-omics, mechanical stress, defense response, *α*-linolenic acid metabolism, phenylalanine metabolism

1. Introduction

Oolong tea is highly appreciated by consumers for its distinctive floral and fruity aroma, mellow taste, and complex flavor profile. Among its production processes, the shaking procedure is a critical step that shapes these characteristic flavors. During shaking, tea leaves are subjected to repeated mechanical stress, triggering a series of metabolic changes that ultimately influence the final quality and aroma of the tea. Importantly, plants have developed inheritable defense-signaling mechanisms to adapt to environmental stresses. The metabolic reactions induced by shaking during oolong tea production exemplify this adaptive mechanism. Various metabolites formed during plant defense responses not only confer resistance to environmental stress, but also constitute essential components of flavor and aroma profiles in numerous plant species (Beck *et al.* 2014). Recent studies have extensively investigated plant reactions to abiotic stresses, with mechanical stress identified as a significant environmental factor. When plants experience mechanical stress, DAMPs transmit stress signals to distal tissues electrical impulses, Ca^{2+} waves, reactive oxygen species (ROS) and hormones, activating both physical and chemical defenses (Choi and Klessig 2016; Huber and Bauerle 2016; Zhang *et al.* 2022). Glutathione mitigates mechanical stress-induced oxidative damage by scavenging excess ROS, thereby protecting plant cells and enhancing self-repair mechanisms *via* redox-homeostasis regulation (Dorion *et al.* 2021). Under abiotic stress, plants precisely regulate the biosynthesis, transport, and metabolism of jasmonates (JAs) — lipid-derived compounds that include jasmonic acid (JA) and its active derivatives jasmonoyl-isoleucine (JA-Ile) and methyl jasmonate (MeJA). This regulation leads to rapid JA and JA-Ile accumulation in wounded tissues, which activates downstream secondary metabolism-related genes and subsequently enhances the production of defense-related compounds, including terpenoids, phenolics, and flavonoids (Zhang *et al.* 2024). These specialized metabolites not only aid stress adaptation but also critically determine flavor through the biosynthesis of volatile organic compounds (VOCs) (Ruan *et al.* 2019).

In recent years, attention has focused on improving plant quality by utilizing defense responses, with tea (*Camellia sinensis* (L.) *O. Kuntze*) serving as a paradigm. Particularly, tea quality can be enhanced through various stress factors applied before and after harvest (Zeng *et al.* 2019b). Oolong tea processing is intricate and shaped by multiple stresses, including light, temperature, dehydration, and mechanical stress. Zuoqing, a key procedure to oolong tea quality, involves repeated cycles of shaking and spreading. Shaking primarily imparts slight mechanical stress to the leaves (Wu *et al.* 2022). These factors modulate the chemical composition and metabolism, ultimately determining oolong tea's distinctive aroma and mellow taste. Studies show that during post-harvest processing—especially physical operations like shaking—JA content and the expression of its biosynthetic genes are significantly up-regulated, further inducing synthesis of specific aroma compounds (Shi *et al.* 2015). External stresses such as mechanical shaking also enhance the transformation of flavor substances including phenylpropanoids, flavonoids, and phenylalanine (Wu *et al.* 2022; Chen *et al.* 2024). Notably, this phenomenon is not limited to oolong tea; during black tea processing, shaking likewise enhances floral and fruity aromas, underscoring the universal role of mechanical stress in aroma formation across tea types (Lin *et al.* 2022). However, previous research has mainly focused on quality-formation mechanisms or functional validation of individual genes, with relatively few studies examining overall responses of tea leaves to mechanical stress through multi-omics analyses.

This study aims to elucidate response mechanisms of tea leaves to mechanical stress during oolong tea production and its impact on quality and flavor formation. Using metabolomic (MB), transcriptomic (TX), and proteomic (PT) analyses, we investigated leaf responses to mechanical stress and examined how these stresses affect formation of key metabolites underlying oolong tea's unique flavor. Our findings advance understanding of flavor-formation mechanisms in oolong tea and provide valuable references

for other tea processing techniques.

2. Materials and methods

2.1. Plant materials and treatments

Tea leaves were plucked from *Camellia sinensis* 'Tieguanyin' cultivated at the tea plantation of Fuqing Nanhushan Co., Ltd., (25°71´N, 119°25´E, Fuzhou, China), consisting of 3 banjhi leaves and an apical bud. Fresh tea leaves (100 kg) were collected and transported to the tea processing facility (temperature 22.0±0.4°C, humidity 83.8±2%). The freshly harvested tea leaves were withered for 45 min. A subset of the withered leaves was designated as the control group (C0). The remaining leaves were randomly divided into 2 equal portions to ensure uniformity between treatment groups. One portion underwent mechanical shaking treatment and was sampled at 15 min (V15). Shaking was conducted using a mechanical vibration Yaoqing platform with the following specifications: table size 1.1 m×1.2 m, fixed amplitude 0.025 m, power 2.2 kW, vibration frequency 330 r min^{-1}, maximum load 100 kg, maximum current 5 A, and voltage 220 V. To minimize background interference, a corresponding batch of withering-only leaves was sampled at the same point (C15). The second leaves from all treatment groups were immediately collected, frozen in liquid nitrogen, and stored at –80°C for furtheranalysis. All treatments were performed with 3 biological replicates.

2.2. Extraction and quantification of volatile components

Volatile metabolites absolute quantification was performed on C0, C15, and V15 samples, each with 3 biological replicates (n=3). Volatile aroma compounds were extracted from 500 mg of finely ground fresh tissue, following the protocol by Zeng *et al.* (2019a) with minor modifications. Dichloromethane (3 mL) was used as the extraction solvent, and ethyl *n*-decanoate (5 nmol) was added as the internal standard. The mixture was vortexed, shaken overnight, dried over anhydrous sodium sulfate, and concentrated under nitrogen flow to a final volume of 100–200 µL. A 1 µL aliquot of the concentrated extract was analyzed by gas chromatography-mass spectrometry (GC-MS) using a GC-MS QP2010 SE System (Shimadzu Corporation, Kyoto, Japan) equipped with GCMS solution software (Version 2.72, Shimadzu Corporation, Japan). Separation was performed using a SUPELCOWAX 10 column (30 m×0.25 mm×0.25 µm, Supelco Inc., Bellefonte, PA, USA) with helium as the carrier gas at a flow rate of 1 mL min^{-1}. The oven temperature program was as follows: initial temperature of 60°C (held for 3 min), ramped at 4°C min^{-1} to 240°C, and held for 20 min. MS analysis was conducted in full scan mode (m/z 40–200). Selected aroma compounds were identified by comparison with authentic standards and quantified using calibration curves (peak area *vs*. concentration) based on serial dilutions.

2.3. Identification and quantification of non-volatile compounds

Metabolite extraction and analysis were conducted on 3 biological replicates (n=3) for each tea sample groups (C0, C15, and V15). Lyophilized tea samples were ground using a mixer mill (MM 400, Retsch) equipped with a zirconium oxide bead for 90 seconds at a frequency of 30 Hz. A 100 mg portion of the powdered sample was extracted overnight at 4°C with 0.6 mL of 70% aqueous methanol. After centrifugation (10,000×g, 10 min), the supernatant was collected and filtered for UPLC-MS/MS analysis. Widely targeted metabolomics was performed using a UPLC-ESI-MS/MS system (AB Sciex), following the method described by Cao *et al.* (2020). Detection was carried out on the UPLC/MS/MS system in MRM mode, with nitrogen as the collision gas at 5 psi. MRM transitions were monitored per acquisition window based on the elution of metabolites. Data analysis, including peak detection, alignment, quantification, and differential metabolite identification, was performed using Analyst 1.6.1 software.

2.4. RNA-sequencing analysis

RNA was extracted from 3 biological replicates (n=3) of each tea sample — C0, C15, and V15 — using the TIANGEN RNAprep Pure Kit (TIANGEN, Beijing, China). RNA integrity and concentration were evaluated as described by Cao *et al.* (2020). Sequencing libraries were prepared from 1.5 µg of total RNA per sample with the NEBNext Ultra RNA Library Prep Kit (NEB, USA) and sequenced on an Illumina HiSeq platform to generate paired-end reads. Raw FASTQ files were processed with in-house Perl scripts to remove adapters, poly-N sequences, and low-quality reads, generating clean reads, allowed by quality metric analysis (Q20, Q30, GC content, duplication rate). Clean reads were assembled with Trinity (Grabherr *et al.* 2011) using a minimum k-mer coverage of 2. Gene expression levels were quantified with RSEM (Li and Dewey 2011), and differential expression was assessed with the DESeq R package (Love *et al.* 2014).

2.5. Protein identification and quantification

Protein extraction and labeling were performed on 3 biological replicates (n=3) for C0, C15, and V15. Leaf powder (ground in liquid nitrogen) was mixed with 4 volumes (w/w) of lysis buffer (8 mol L^{-1} urea, 1% Triton X-100, 10 mmol L^{-1} DTT, 1% protease inhibitor) and sonicated on ice for 3 cycles. After centrifugation (20,000×g, 10 min, 4°C), proteins in the supernatant were precipitated with 20% TCA, washed 3 times with cold acetone, redissolved in 8 mol L^{-1} urea, and quantified with a BCA kit. Proteins were reduced with 5 mmol L^{-1} DTT (56°C, 30 min), alkylated with 11 mmol L^{-1} iodoacetamide (dark, 25°C, 15 min), and diluted to <2 mol L^{-1} urea. Sequential trypsin digestion (1:50 w/w overnight; 1:100 w/w for 4 h) was followed by C18 desalting and lyophilization. Peptides were labeled with iTRAQ reagents (0.5 mol L^{-1} TEAB, 25°C, 2 h), pooled, desalted, and separated on an EASY-nLC 1000 UPLC System (15 cm C18 column, 400 nL min^{-1}) with a gradient of 6–23% acetonitrile (0.1% formic acid) for 26 min, 23–35% in 8 min, 35–80% in 3 min, and held at 80% for 3 min. NSI-MS/MS analysis (Q Exactive Plus) was performed at MS^1 resolution 70,000 and MS^2 resolution

17,500 (28% collision energy). Data were processed with MaxQuant against the *Camellia sinensis* var. *shuchazao* genome (Wei *et al.* 2018). Functional annotation used UniProt-GOA and KAAS databases.

2.6. Quantitative real-time PCR analysis

To validate the transcriptome data reliability, a total of 10 genes were selected for qRT-PCR. Total RNA was reverse-transcribed with a commercial kit and amplified using SYBR Premix *Ex Taq* II (TaKaRa, Japan) on a CFX96 system (Bio-Rad). Relative expression levels were calculated by the $2^{-\Delta\Delta CT}$ method, using *CsPTB1* as the internal control (Hao *et al.* 2014). Each reaction was performed in triplicate. Primer sequences are listed in Appendix A.

2.7. Date analysis

For each sample, 3 biological replicates were analyzed for MB, TX, and PT assays. Principal component analysis (PCA) was conducted with Origin 2021 (OriginLab Corporation, USA). Statistical tests were performed with SPSS (SPSS Inc., USA) and GraphPad Prism 7 (GraphPad Software Inc., USA). Group differences were assessed by two-tailed Student's *t*-test (α=0.01). Differential volatile metabolites and non-volatile metabolites were evaluated by VIP>1, P<0.05, and fold change>1.2 or <1/1.2. Significant KEGG pathways were identified at FDR≤0.05. Differentially expressed genes (DEGs) were identified by $|\log_2 FC| \geq 1$ and P<0.05. Differentially expressed proteins (DEPs) were screened with fold change>1.2 or <1/1.2 and adjusted P<0.05. Pathway enrichment analysis employed Fisher's exact test with FDR<0.05 as the significance threshold.

3. Results

3.1. Changes in volatile metabolites in tea leaves under mechanical stress

Volatile compounds in tea samples were identified and quantified using GC-MS, based on comparisons with authentic standards. A total of 18 metabolites were identified and quantified through absolute quantification. PCA revealed that PC1 and PC2 collectively accounted for 85.0% of the total variance (PC1, 55.4%; PC2, 29.6%). Additionally, replicates of each sample clustered tightly, and clear separation was observed among different treatment groups (Fig. 1-A). These results suggest that metabolite profiles were influenced by

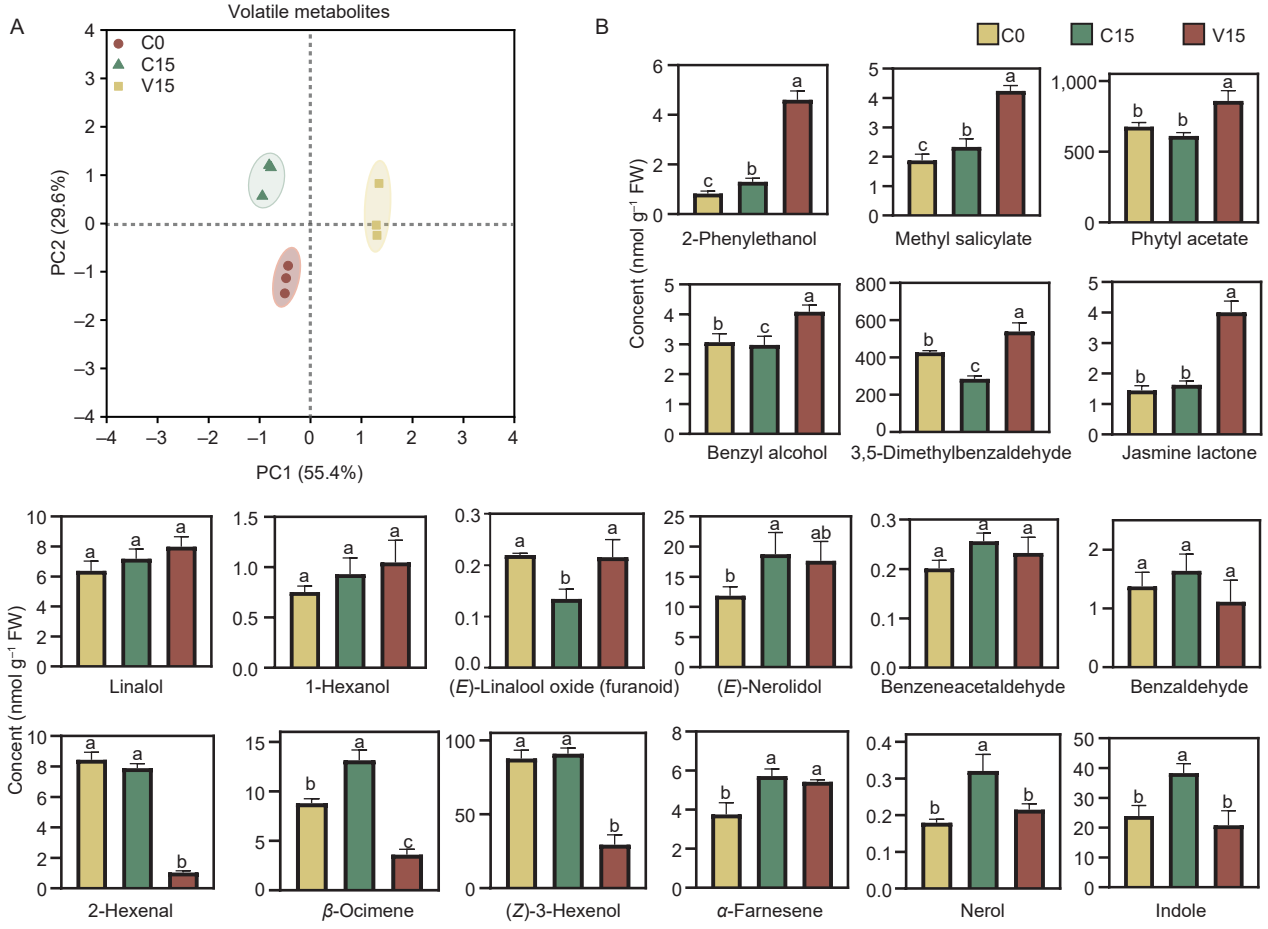


Fig. 1 Volatile metabolite profiles of tea samples under different treatments. A, principal component analysis (PCA) showing the clustering of volatile metabolites under different treatments. B, absolute concentrations of 18 characteristic volatile compounds across 3 treatments (C0, C15 and V15). C0, withered leaves; C15, withered leaves subjected to an additional 15 min of withering; V15, withered leaves subjected to mechanical stress for 15 min. FW, fresh weight. Different lowercase letters (a, b, c) above bars indicate significant differences (P<0.05).

stress during oolong tea processing, particularly mechanical stress. Fig. 1-B and Table 1 present the absolute quantitative data, including concentrations, statistical significance, retention indices (RI), odor descriptions, and dynamic changes of detected volatiles. Among these 18 volatile metabolites, a total of 8 were differentially regulated in both the V15 *vs.* C0 and V15 *vs.* C15 comparisons, based on criteria of VIP>1, $P<0.05$, and fold change>1.2 or <1/1.2 (Appendix B). Notably, a total of 6 compounds exhibited significantly elevated concentrations in V15 compared to both control groups (C0 and C15), indicating a strong stimulatory effect of mechanical stress. For example, 2-phenylethanol (rose-like, fruity) increased to 4.6088 nmol g^{-1} in V15, representing an approximately 5.6-fold increase over C0 (0.8285 nmol g^{-1}) and a 3.5-fold increase over C15 (1.3004 nmol g^{-1}). Methyl salicylate (minty, floral) increased to 4.2383 nmol g^{-1} in V15, a 2.3-fold increase compared to C0 (1.8725 nmol g^{-1}) and a 1.8-fold increase over C15 (2.3322 nmol g^{-1}). 3,5-Dimethylbenzaldehyde (herbaceous, vanilla-like) increased to 539.1502 nmol g^{-1} in V15, higher than both C0 (427.8438 nmol g^{-1}, ~1.3-fold increase) and C15 (285.7551 nmol g^{-1}, ~1.9-fold increase). Benzyl alcohol (rose-like and fruity) increased to 4.0873nmol g^{-1} in V15, increased from C0 (3.0717 nmol g^{-1}, ~1.3-fold) and C15 (2.9790 nmol g^{-1}, ~1.4-fold). Phytol acetate (floral, fruity) increased to 860.0508 in V15, surpassing C0 (677.1109 nmol g^{-1}, ~1.3-fold) and C15 (611.1156 nmol g^{-1}, ~1.4-fold). Jasmine lactone (creamy) increased to 4.0083 in V15, marking a 2.8-fold increase over C0 (1.4472 nmol g^{-1}) and a 2.5-fold increase over C15 (1.6291 nmol g^{-1}). In contrast, concentrations of green-note compounds decreased substantially. For instance, 2-Hexenal (green, lipid-derived aldehyde) declined sharply to 1.04 nmol g^{-1} in V15, down from 8.45 nmol g^{-1} in C0 and 7.89 nmol g^{-1} in C15. (*Z*)-3-Hexenol (green, grassy), another key green aroma contributor, decreased to 29.47 nmol g^{-1} in V15, compared to 87.69 nmol g^{-1} in C0 and 91.04 nmol g^{-1} in C15. These reductions suggest that mechanical stress may promote degradation or transformation of green-note volatiles, thereby diminishing the grassy aroma in the final product.

3.2. Changes in non-volatile metabolites in tea leaves under mechanical stress

To assess alterations in non-volatile metabolites under mechanical stress, a widely-targeted metabolomics analysis was performed on withered tea leaves (C0) and 2 treated samples (C15 and V15). As a result, a total of 772 non-volatile metabolites were identified and quantified. PCA revealed clear separation among tea samples based on treatment, with tight clustering among technical replicates (Fig. 2-A). The first two principal components accounted for 58.73% of total variance—42.42% from PC1 and 16.31% from PC2.

Differentially regulated non-volatile metabolites (DRNs) were identified based on VIP>1, $P<0.05$, and fold change>1.2 or <1/1.2 (Appendix C). Mechanical stress (V15 group) significantly altered the metabolic profile. Compared with the control group (C0), 121 metabolites showed significant changes in V15, including 95 upregulated and 26 downregulated metabolites. In the V15 *vs.* C15 comparison, 87 differential metabolites were identified, including 82 upregulated and 5 downregulated. In contrast, only 14 metabolites significantly differed between C15

Table 1 Absolute levels of volatile metabolites in C0, C15, and V15 tea samples

Number	Volatile compounds	CAS[1)]	Odour description	R (min)[2)]	RI[3)]	Absolute quantification (nmol g^{-1} FW)[4)]		
						C0±STD	C15±STD	V15±STD
1	2-Hexenal	505-57-7	Grassy, herbal	8.775	1,216	8.4457±0.4948 a	7.8931±0.2891 a	1.0449±0.1023 b
2	*β*-Ocimene	13877-91-3	Floral	9.79	1,250	8.7981±0.4602 b	13.1329±1.0522 a	3.6101±0.5356 c
3	1-Hexanol	111-27-3	Herbal	12.75	1,344	0.7542±0.0574 a	0.9308±0.1614 a	1.0475±0.2208 a
4	(*Z*)-3-Hexenol	928-96-1	Green, grassy	13.765	1,375	87.6875±5.6700 a	91.0363±3.7470 a	29.4677±6.6056 b
5	(*E*)-Linalool oxide (furanoid)	34995-77-2	Floral	15.8	1,438	0.2198±0.0031 a	0.1342±0.0190 b	0.2156±0.0341 a
6	Benzaldehyde	100-52-7	Fruity, almond	18.43	1,519	1.3755±0.2414 a	1.6385±0.2869 a	1.1142±0.3658 a
7	Linalol	78-70-6	Floral	19.2	1,543	6.3827±0.6503 a	7.1811±0.6485 a	7.9822±0.6737 a
8	Benzeneacetaldehyde	122-78-1	Sweet, floral	22.17	1,654	0.2010±0.0166 a	0.2561±0.0167 a	0.2326±0.0314 a
9	*α*-Farnesene	502-61-4	Floral	25.545	1,762	3.7591±0.5971 b	5.7272±0.3538 a	5.4261±0.1102 a
10	Methyl salicylate	119-36-8	Minty, floral	26.2	1,780	1.8725±0.2161 c	2.3322±0.2748 b	4.2383±0.1852 a
11	3,5-Dimethylbenzaldehyde	5779-95-3	Herb, vanilla	27.325	1,813	427.8438±8.6351 b	285.7551±14.8145 c	539.1502±46.8475 a
12	Nerol	106-25-2	Floral, orange	28.115	1,841	0.1792±0.0095 b	0.3209±0.0450 a	0.2151±0.0160 b
13	Benzyl alcohol	100-51-6	Rose-like, fruity	28.85	1,868	3.0717±0.2798 b	2.9790±0.2859 c	4.0873±0.2269 a
14	2-Phenylethanol	60-12-8	Rose-like, fruity	29.835	1,904	0.8285±0.0969 c	1.3004±0.1404 b	4.6088±0.3512 a
15	Phytol, acetate	10236-16-5	Floral, fruity	30.675	1,935	677.1109±28.8913 b	611.1156±23.8339 b	860.0508±72.1592 a
16	(*E*)-Nerolidol	40716-66-3	Floral, fruity	33.43	2,041	11.8542±1.4763 b	18.7289±3.6076 a	17.6334±3.2166 ab
17	Jasmine lactone	25524-95-2	Creamy	38.855	2,263	1.4472±0.1546 b	1.6291±0.1276 b	4.0083±0.3641 a
18	Indole	120-72-9	Camphor	42.94	2,445	23.9295±3.5230 b	38.3244±3.1827 a	20.8292±4.8445 b

[1)] CAS, chemical abstracts service registry number.
[2)] R, retention time (min).
[3)] RI, retention index.
[4)] Metabolite contents determined by standard curve method. Unit: nanomoles per gram fresh weight (FW) (nmol g^{-1} FW). C0, withered leaves; C15, withered leaves subjected to an additional 15 min of withering; V15, withered leaves subjected to mechanical stress for 15 min. Data are mean±SD (n=3). Significant differences among various groups are represented by different letters ($P<0.05$)

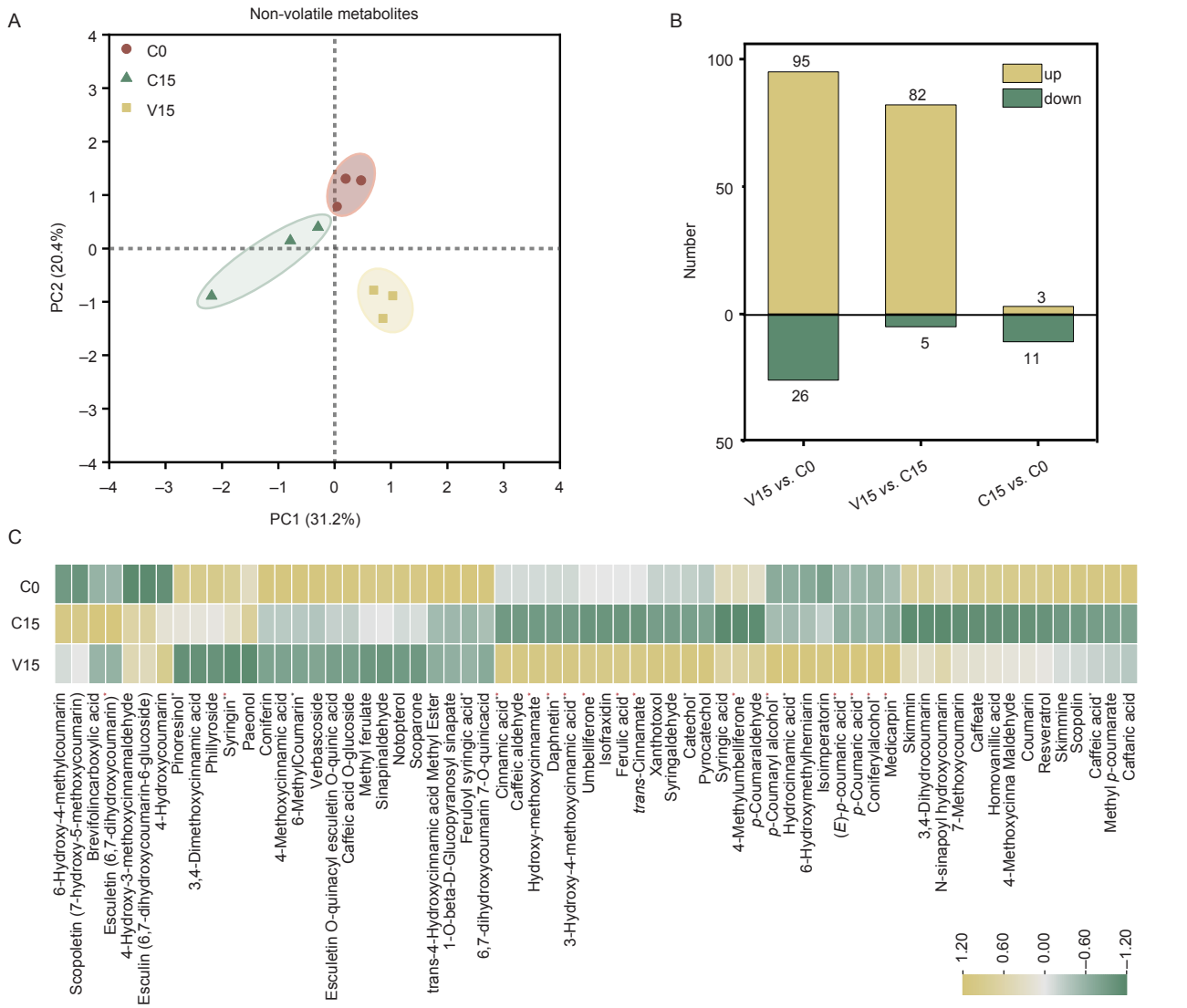


Fig. 2 Non-volatile metabolites profiles of tea samples under different treatments. A, PCA demonstrating the clustering of non-volatile metabolites under different treatments (C0, C15 and V15). B, the number of significant differential metabolites in each paired comparison. C, heat map of phenylpropanoids in tea samples, where black (˙) indicates significant differences between V15 and C0, and a red (˙) indicates significant differences between V15 and C15, with selection criteria of P<0.05 and VIP≥1. C0, withered leaves; C15, withered leaves subjected to an additional 15 min of withering; V15, withered leaves subjected to mechanical stress for 15 min.

and C0 (3 upregulated and 11 downregulated) (Fig. 2-B), indicating mechanical stress as the primary driver of metabolic reprogramming. To further investigate the effects of mechanical stress, KEGG pathway enrichment analysis was performed for both V15 *vs.* C0 and V15 *vs.* C15. A total of 7 metabolic pathways were commonly enriched in both comparisons, including phenylpropanoid biosynthesis, isoflavonoid biosynthesis, purine metabolism, biosynthesis of secondary metabolites, general metabolic pathways, *β*-alanine metabolism, and ubiquinone and other terpenoid-quinone biosynthesis (Appendix D). These findings suggest that V15 treatment specifically modulates critical pathways in both primary and secondary metabolism. Furthermore, lipids, nucleotides, and their derivatives accumulated significantly after mechanical stress, and levels of various secondary metabolites, such as phenylpropanoids and amino acid derivatives, also changed notably (Appendix E). Phenylpropanoid-related metabolites showed significant regulation. In both V15 *vs.* C0 and V15 *vs.* C15 comparisons, 15 differential metabolites were identified, with 9 commonly altered. These include *p*-coumaric acid, cinnamic acid, (*E*)-*p*-coumaric acid, 3-hydroxy-4-methoxycinnamic acid, syringetin, abietinol, medicarpin, *p*-coumaryl alcohol, and anethole (Fig. 2-C). These consistently altered metabolites may play crucial roles in the regulatory response to mechanical stress.

3.3. Changes in transcriptomic profiles in tea leaves under mechanical stress

To gain deeper insights into the molecular responses to mechanical stress, a transcriptomic analysis was conducted to investigate how tea leaves respond to such stimuli. RNA sequencing was performed on the Illumina platform for C0, C15, and V15 groups, each with 3 biological replicates, yielding an average of 8.89 Gb of clean data per sample.

PCA of the transcriptomic data showed clear separation of C0, C15, and V15 samples, with biological replicates clustering. The first two principal components explained 51.9% of the variance (PC1: 30.7%, PC2: 21.3%) (Fig. 3-A).

To assess the transcriptional impact of different treatments, differentially expressed genes (DEGs) were identified using the criteria $|\log_2 FC| \geq 1$ and $P<0.05$. The number of DEGs varied across the V15 *vs.* C0, V15 *vs.* C15, and C15 *vs.* C0 comparisons, with 2,313, 1,124, and 330 DEGs identified, respectively. The V15 *vs.* C0 group exhibited the most extensive regulation, including 1,604 upregulated and 709 downregulated genes, accounting for 5.46% of all detected genes (Fig. 3-B). KEGG enrichment analysis was conducted to elucidate the biological functions of DEGs, and the top 8 significantly enriched pathways were identified (Fig. 3-C). Notably, DEGs induced by mechanical stress were enriched in pathways such as glutathione metabolism, *α*-linolenic acid metabolism, and the biosynthesis of secondary metabolites pathway. In addition, the V15 *vs.* C15 comparison showed significant enrichment in the phenylpropanoid biosynthesis pathway, indicating that mechanical stress may activate multiple defense-related pathways in tea leaves and promotes the accumulation of secondary metabolites.

To identify DEGs specifically induced by mechanical stress rather than dehydration stress, Venn diagram analysis was performed, identifying 792 mechanically induced genes (MIGs). Metascape analysis of the top 14 significantly enriched GO terms for these MIGs (Fig. 3-D) revealed strong intra- and inter-category relationships, forming 4 distinct clusters. Among these, a total of 8 GO terms related to mechanical stress were highly interconnected, including MAPK signaling pathway, response to wounding, plant hormone signal transduction, plant-pathogen interaction, toxin metabolic process, defense response to fungus, response to bacterium, response to oxidative stress, and response to light stimulus. These results suggest that mechanical stress activates multiple signal transduction pathways involved in plant defense responses. To validate the transcriptomic findings, qRT-PCR was conducted on 10 DEGs selected from RNA-seq data. The qRT-PCR results showed trends consistent with the RNA-seq data, confirming the reliability of the transcriptome analysis (Appendix F).

3.4. Changes in protein abundance in tea leaves under the mechanical stress

To further elucidate the mechanisms triggered by mechanical stress, a TMT-based proteomic analysis was conducted on 3 closen groups: C0, C15, and V15. A total of 7,337 proteins were identified, of which 6,244 were quantified. The results revealed distinct differences in protein abundance among the treatments, indicating significant alterations in protein expression patterns across groups (Fig. 4-A). Pairwise comparisons between V15 *vs.* C0, V15 *vs.* C15 and C15 *vs.* C0 showed varying numbers of DEPs (Fig. 4-B), identified based on fold change>1.2 or <1/1.2 and adjusted $P<0.05$. The V15 *vs.* C0 comparison yielded the highest number of DEPs, including 301 upregulated and 65 downregulated proteins, suggesting that mechanical stress substantially alters the tea leaf proteome.

To identify proteins specifically responsive to mechanical stress rather than dehydration, a Venn diagram analysis was performed. This analysis revealed 47 mechanically induced proteins (MIPs) (Fig. 4-C), indicating that mechanical stress may activate specific signaling pathways or molecular mechanisms not engaged during dehydration stress. KEGG pathway enrichment analysis of MIPs revealed significant enrichment in pathways including 'Metabolic pathways', 'Protein processing in the endoplasmic reticulum', 'Biosynthesis of secondary metabolites', 'Phenylpropanoid biosynthesis', and 'Autophagy' (Fig. 4-D). These results underscore the involvement of mechanical stress in modulating both primary metabolism and stress-related processes.

3.5. Multi-omics analysis of damage-associated molecular patterns in tea leaves

Damage-associated molecular patterns (DAMPs) are endogenous molecules released by plant cells under abiotic stress, which initiate signaling cascades to activate defense responses (Hou *et al.* 2021). To further elucidate the molecular characteristics of DAMPs in postharvest tea leaves, multi-omics analyses — metabolomics (MB), transcriptomics (TX), and proteomics (PT), were performed on C0, C15, and V15 samples. Mechanical stress was found to activate multiple defense signaling pathways in tea leaves, with the associated genes and their encoded proteins exhibiting coordinated upregulation or downregulation patterns (Fig. 5-A). As shown in Fig. 5-B, several *CNGCs* genes and their corresponding proteins were significantly upregulated in V15, indicating enhanced expression and accumulation of cyclic nucleotide-gated channel (CNGC) proteins under mechanical stress. Elevated intracellular Ca^{2+} levels subsequently triggered downstream signaling cascades, including the activation of *CaCML* genes and their encoded proteins, which in turn stimulated nitric oxide synthase (NOS) activity, leading to nitric oxide (NO) accumulation and the initiation of a defense response. In parallel, Ca^{2+} signaling also facilitates the production of reactive oxygen species (ROS) by activating *CDPK*, *Robh*, and their encoded proteins.

In the V15 groups, the upregulation of *FLS2*, *a* gene encoding a receptor associated with plant innate immunity, along with its protein product, supports the crucial role of ROS in defense signaling. Although *MEKK1* and *MKK4* genes showed a downregulation trend, the upregulation of MKK proteins suggested activation of downstream signaling components such as *MPK3/6*, *WRKY22*, and their respective proteins, which are key regulators of ROS production and stress adaptation. Under mechanical stress, the *RIN4* gene and its encoded protein were activated, leading to upregulation of *HSP90*, a heat shock protein involved in immune signaling. Key immune receptors, including *RPM1* and *RPS2*, also showed elevated expression, with 17 *RPM1* genes being upregulated, suggesting that mechanical stress triggers robust activation of immune signaling pathway. Furthermore, *PBS1*, a gene involved in membrane receptor signaling, showed partial upregulation, contributing

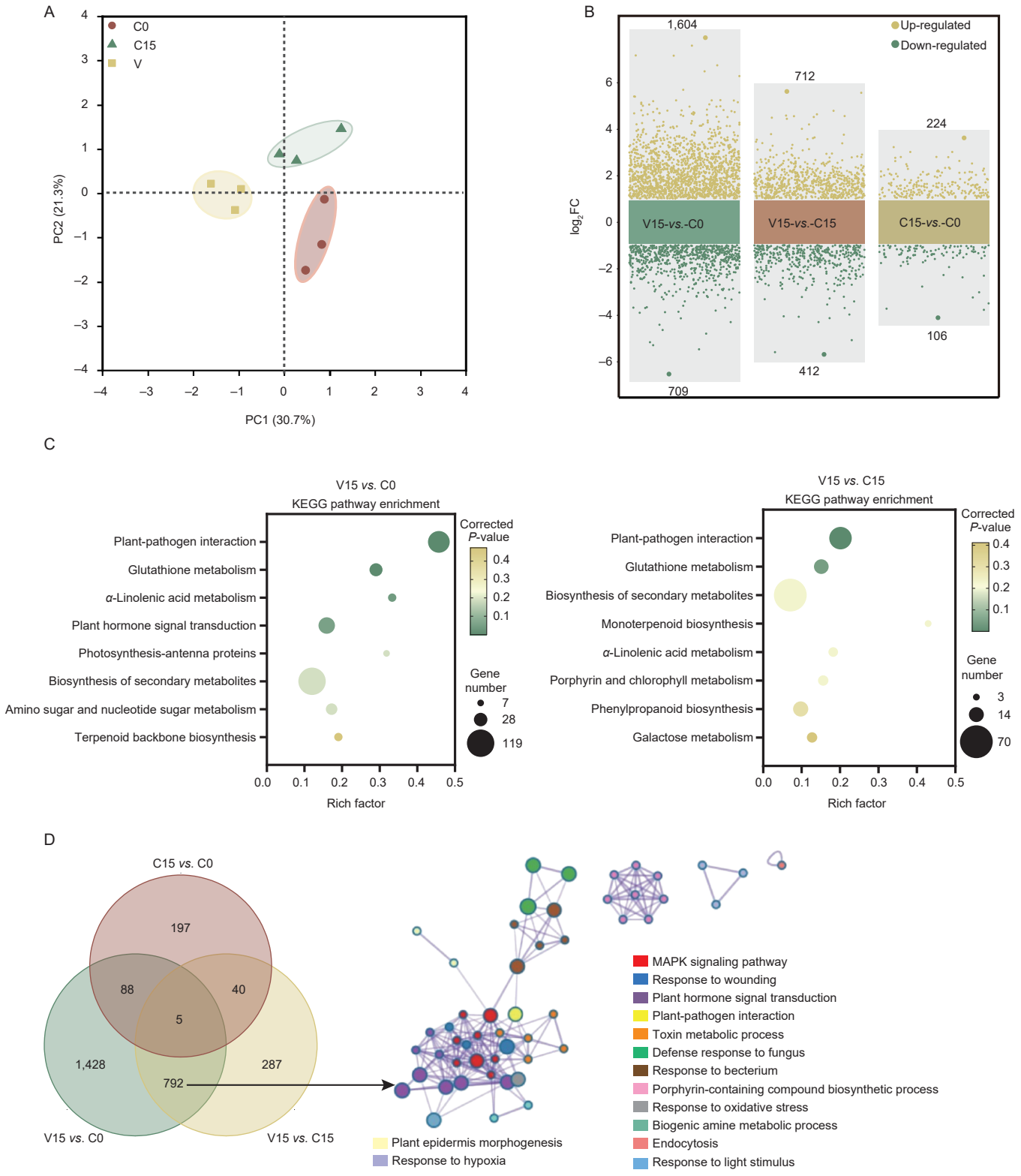


Fig. 3 Transcriptomic profiles of tea samples subjected to various treatments. A, PCA score plot of transcriptomic profiles for tea samples. B, the number of significantly differentially expressed genes (DEGs) in various paired-comparisons of tea samples. Each point in the plot represents a significant DEG. The numbers labeled on each comparison indicate the number of downregulated or upregulated express genes. C, KEGG enrichment analysis of DEGs between C0, C15, and V15. P<0.05 and rich factor=the ratio of DEGs in this pathway to the total number of genes in the pathway. The circle size reflects the gene count, while the x-axis (rich factor) represents the pathway's enrichment level. D, GO enrichment analysis of mechanically induced genes (MIGs). GO enrichment analysis was conducted using the Metascape web platform. Each circle dot represented a GO term. Representative circle dots are converted into a network layout and the thickness of the edge represents the similarity score between terms. C0, withered leaves; C15, withered leaves subjected to an additional 15 min of withering; V15, withered leaves subjected to mechanical stress for 15 min. FC, fold change.

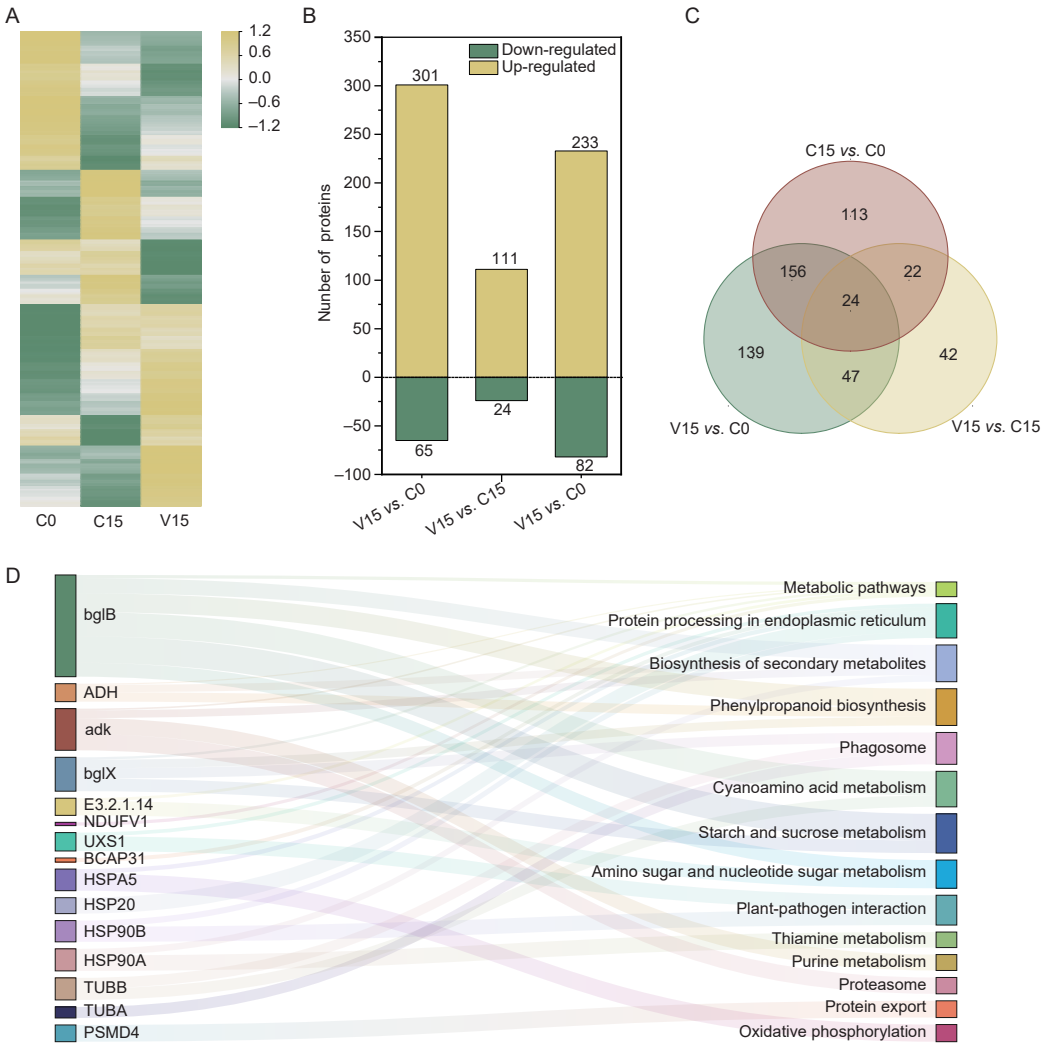


Fig. 4 Proteomic profiles of tea samples under different treatments. A, a heat map showing the abundance of proteomic profiles across different tea samples. B, the number of significantly differentially expressed proteins (DEPs) identified in pairwise comparisons among the tea samples. C, Venn diagram of different proteins between comparison groups. D, KEGG pathway enrichment analysis of mechanically induced proteins (MIPs).

to the enhanced expression of *RPS5*, another immune receptor. The JA signaling pathway plays a pivotal role in tea leaf responses to mechanical stress and regulates the biosynthesis of volatile compounds. The key gene *COI1*, a JA receptor, exhibited downregulation at the transcript level, while its corresponding protein was upregulated, suggesting a temporal lag between gene expression and protein accumulation. Additionally, *JAZ*, a repressor of JA signaling, was significantly upregulated, and its downstream factor *MYC2* showed partial upregulation, confirming activation of the JA signaling cascade.

Mechanical stress also triggered the accumulation of NO and ROS, leading to activation of the glutathione metabolism pathway (Fig. 5-A). This was consistent with KEGG enrichment pathway analysis, which showed significant enrichment of DEGs and DEPs within the glutathione metabolism pathway. This indicates that this pathway plays a role in maintaining redox balance and contributing to tea quality formation. As shown in Fig. 5-C, gene expression, protein abundance, and metabolite levels displayed generally consistent trends under mechanical stress. Several key redox-related genes, including *6PGDp*, *GPX*, and *GSTU*, *were* upregulated, while *APX*, as well as genes involved in glutathione biosynthesis such as *GSH1* and *GSH2*, were downregulated. These transcriptional changes were accompanied by corresponding protein expression patterns and metabolite fluctuations. Notably, *GPX* and its encoded protein were upregulated in V15 samples, and 22 out of 23 *GST* genes also showed increased expression, along with partial upregulation of GST proteins.

At the metabolite level, a decrease in GSH and an increase in GSSG were observed, likely reflecting oxidation of GSH during ROS scavenging. The ascorbate-glutathione (ASC-GSH) cycle, a central component of the antioxidant system, also showed notable changes. ASC levels declined, and *APX* gene expression was downregulated (Fig. 5-A), although APX protein abundance showed partial upregulation. This discrepancy may result from transcriptional repression

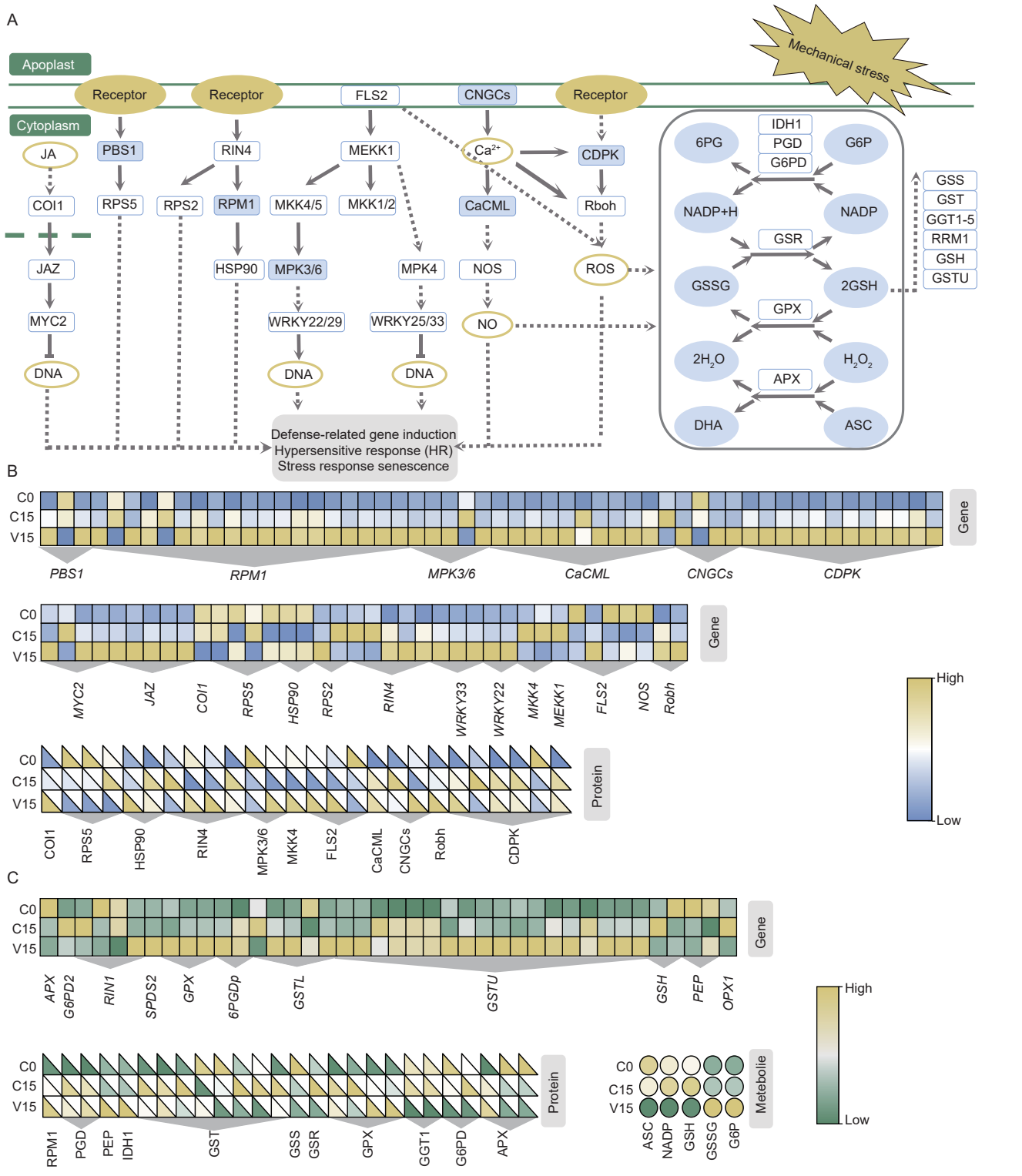


Fig. 5 Integrated visualization of metabolite, gene, and protein abundance within biochemical network pathway maps. A, pathway map of damage-associated molecular patterns (DAMPs). B, heat maps derived from metabolomics (MB), transcriptomics (TX), and proteomics (PT) datasets related to signal transduction pathways. C, heat maps derived from MB, TX, and PT datasets related to the glutathione metabolism pathway (gray box). CNGCs, cyclic nucleotide-gated channels; CaCML, calmodulin-like proteins; CDPK, calcium-dependent protein kinase; Rboh, respiratory burst oxidase homolog; MPK, mitogen-activated protein kinase; MEKK, mitogen-activated protein kinase kinase kinase; MKK, mitogen-activated protein kinase kinase; RIN4, resistance to pseudomonas syringae 4; RPM1, resistance to pseudomonas syringae pv. maculicola 1; HSP90, heat shock protein 90; RPS, ribosomal protein S; PBS1, AvrPphB susceptible 1; COI1, coronatine insensitive 1; JAZ, jasmonate ZIM-domain; MYC2, basic helix-loop-helix transcription factor; IDH1, isocitrate dehydrogenase 1; PGD, phosphogluconate dehydrogenase; GSR, glutathione reductase; GPX, glutathione peroxidase; APX, ascorbate peroxidase; GSS, glutathione synthetase; GSTU, glutathione S-transferase Tau; GST, glutathione S-transferase; GGT1-5, gamma-glutamyltransferase 1-5.

combined with post-translational stabilization of APX protein to maintain antioxidant capacity under mechanical stress. In summary, mechanical stress activates the release of DAMPs in tea leaves, triggering multiple immune and antioxidant signaling pathways that coordinate transcript, protein, and metabolite responses to mitigate damage and preserve cellular function.

3.6. Revealing quality-related metabolic mechanisms in tea leaves under mechanical stress through multi-omics analysis

Mechanical stress modulates the accumulation of key quality-related metabolites in tea leaves. In V15, levels of α-linolenic acid and its biosynthetic precursor phosphatidylcholine were significantly increased, along with the upregulation of biosynthetic genes such as *SDP1* and *DAD1* (Fig. 6-A). KEGG enrichment analysis showed that the α-linolenic acid metabolism pathway was significantly enriched in both the V15 *vs.* C0 and V15 *vs.* C15 comparisons (Fig. 3-D). A coordinated upregulation was observed at the metabolite, transcript and protein levels in V15, with key genes — including *HPL*, *AOS*, *AOC*, *OPRs*, *OPCL*, and *ACX* and their corresponding proteins exhibiting consistent expression trends (Fig. 6-A). Interestingly, a comparison between withering (C15) and shaking (V15) treatments revealed differential expression patterns for *LOX* genes and their encoded proteins. For example, *LOX2*, *LOX3*, and *LOX6* showed opposite expression trends in the 2 treatments: in C15, these proteins were partially downregulated, whereas in V15, they were upregulated. This trend correlated with α-linolenic acid levels, which increased notably in V15 but remained almost unchanged in C15. These findings suggest that mechanical stress more strongly induces the α-linolenic acid metabolism pathway than dehydration stress alone. Of note, mechanical stress downregulated *ADH1*, which encodes ethanol dehydrogenase, an enzyme responsible for converting 3-hexenal (a grassy odor compound) into 3-hexenol, which contributes to a fresher aroma. This indicates that mechanical stress suppresses *ADH1* expression, thereby limiting the conversion of 3-hexenal to 3-hexenol. This mechanism may explain the presence of a grassy aroma in the early stages of shaking, while withered leaves retain a fresher scent.

Phenylalanine serves as a critical precursor in the biosynthesis of aromatic compounds and flavonoids. In this study, the V15 samples exhibited substantial accumulation of phenylalanine-derived downstream metabolites, including cinnamic acid, *p*-coumaric acid, benzyl alcohol, phenylacetaldehyde, and 2-phenylethanol. To investigate the underlying regulatory mechanisms, an integrated multi-omics analysis of DEGs, DEPs, and DEMs was performed, identifying key molecular components involved in these metabolic pathways (Fig. 6-B). Mechanical stress generally upregulated genes and proteins involved

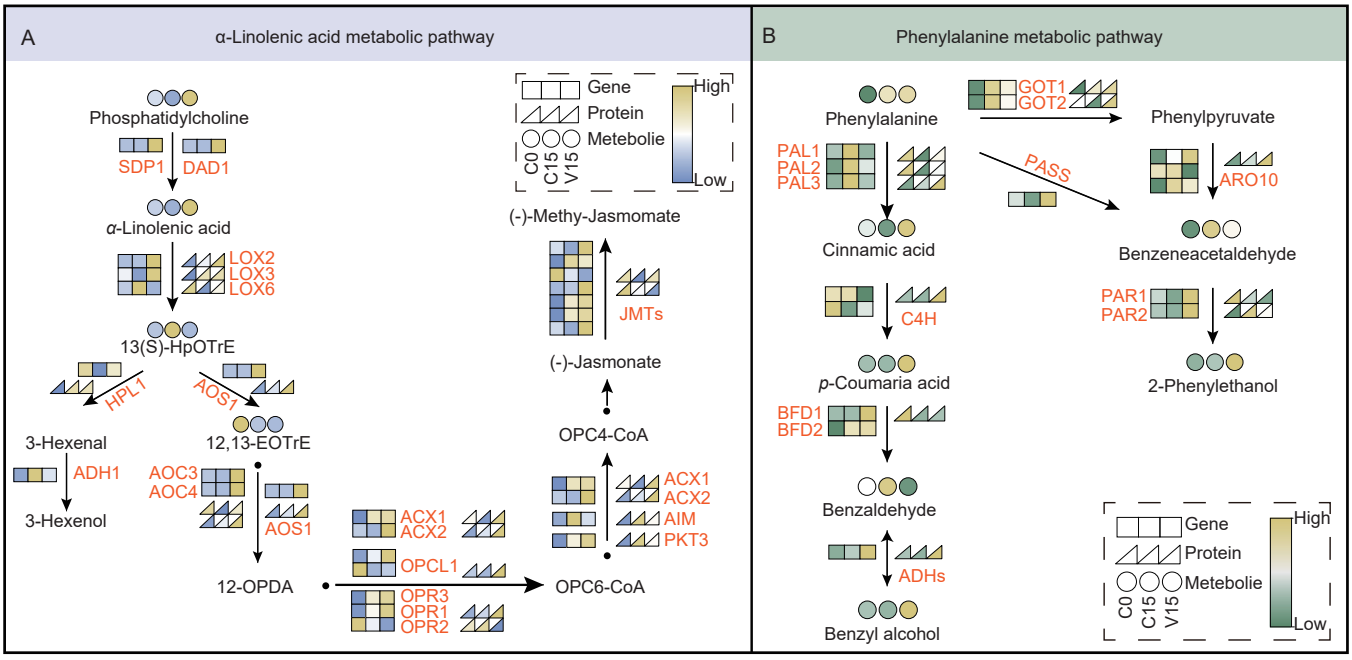


Fig. 6 Visualization of metabolite, gene, and protein abundance in quality-related metabolic pathways. A, simplified models of partial α-linolenic acid metabolic pathways, along with heat maps showing the expression patterns of metabolites, genes, and proteins enriched in these pathways. B, simplified models of partial phenylalanine metabolic pathways, with heat maps depicting the expression patterns of metabolites, genes, and proteins enriched in these pathways. SDP, stearoyl-ACP desaturase; DAD, defective in anther dehiscence 1; LOX, lipoxygenase; HPL, hydroperoxide lyase; AOS, allene oxide synthase; ADH, alcohol dehydrogenase; AOC, allene oxide cyclase; ACX, acyl-CoA oxidase; OPCL, oxygen-dependent phytodienoate reductase-like; OPR, 12-oxophytodienoate reductase; PKT, 3-ketoacyl-CoA thiolase; AIM, aberrant induction of malate; JMTs, jasmonic acid carboxyl methyltransferase. PAL, phenylalanine ammonia-lyase; C4H, cinnamate-4-hydroxylase; BFD, benzoylformate decarboxylase; ADHs, alcohol dehydrogenases; GOT, glutamate oxaloacetate transaminase; PASS, phenylacetaldehyde; ARO10, aromatic decarboxylase; PAR, phenylacetaldehyde reductase.

in the 2-phenylethanol biosynthetic pathway. In the phenylacetaldehyde biosynthesis pathway, both *GOT* and *ARO10*, along with their encoded proteins, were upregulated under both dehydration and mechanical stress conditions. Notably, *PAAS* exhibited specific upregulation in response to mechanical stress, highlighting its stress-responsive role in phenylacetaldehyde synthesis. In V15 samples, the upregulation of *PAR* and its encoded protein product facilitated the reduction of phenylacetaldehyde to 2-phenylethanol. Additionally, elevated levels of cinnamic acid, *p*-coumaric acid, and benzyl alcohol were detected in an alternate branch of the phenylalanine metabolic pathway. The observed upregulation of *ADH* genes and their encoded proteins likely contributed to the enhanced biosynthesis of benzyl alcohol.

4. Discussion

The shaking process is a key procedure in postharvest oolong tea processing and plays a central role in inducing complex physiological responses in tea leaves. In this study, integrated multi-omics analysis revealed that mechanical stress significantly activated JA and calcium signaling pathways, thereby regulating downstream metabolic networks, particularly the *α*-linolenic acid metabolism pathway and the phenylalanine metabolism pathway. These signaling cascades facilitated the accumulation of both volatile and non-volatile compounds, including jasmine lactone, benzyl alcohol, cinnamic acid, and *p*-coumaric acid. These findings provide new insights into how early signaling events orchestrate postharvest metabolic transformations during oolong tea processing.

Mechanical stress during oolong tea processing significantly influenced both volatile and non-volatile metabolite profiles. Previous studies have reported that jasmine lactone accumulates under sustained mechanical stress and contributes notably to the overall aroma profile of oolong tea (Zeng *et al.* 2018; Guo *et al.* 2022). Similarly, 2-phenylethanol and methyl salicylate increase during the shaking process, enhancing floral-fruity notes (Hu *et al.* 2020; Zhou *et al.* 2023). In this study, we observed significant accumulation of these compounds in the V15 samples, supporting the notion that mechanical stress promotes their biosynthesis and contributes to aroma formation. In contrast, 2-hexenal, a volatile with grassy and herbal notes, was significantly reduced, suggesting that shaking facilitates the volatilization or transformation of green aromas—consistent with earlier observations (Wang *et al.* 2000). Non-volatile metabolites also responded sensitively to mechanical stress, aligning with previous studies showing that both mechanical and dehydration stresses regulate tea leaf metabolism (Huang *et al.* 2020; Lin *et al.* 2024). Flavonoids and amino acids are key contributors to tea flavor: amino acids enhance umami and mellowness, while flavonoids provide core taste elements and serve as precursors for important aroma-related metabolites (He *et al.* 2021; Cai and Aharoni 2022). Although recent studies have examined the biosynthesis of flavonoids and amino acids (Huang *et al.* 2020; Wu *et al.* 2022), a detailed understanding of how these pathways dynamically respond to mechanical stress remains limited. Our metabolomic analysis identified 9 phenylpropanoid pathway compounds that significantly accumulated under mechanical stress: *p*-coumaric acid and cinnamic acid, *(E)-p*-coumaric acid, 3-hydroxy-4-methoxycinnamic acid, syringin, coniferyl alcohol, medicarpin, *p*-coumaryl alcohol, daphnetin. Notably, coumarin derivatives — key intermediates in flavonoid biosynthesis — showed pronounced changes, suggesting that mechanical stress enhances phenylalanine metabolism and activates flavonoid pathway, thus contributing to the characteristic mellow taste and rich aroma of oolong tea (Zhang *et al.* 2019; Huang *et al.* 2020; Wu *et al.* 2022).

Previous research has shown that mechanical stress induces dynamic intracellular Ca^{2+} signaling, with *CNGC19* mediating Ca^{2+} influx and triggering downstream defense responses (Meena *et al.* 2019). Elevated Ca^{2+} levels activate *CaCMLs* expression and CaCMLs protein activity, stimulating NOS to produce NO and promote ROS generation through *CDPKs/Rbohs* genes and CDPKs/Rbohs proteins. These signals initiate immune responses, consistent with prior studies identifying CaCMLs and CDPKs as core regulators of Ca^{2+}-dependent signaling (O'Connell *et al.* 2012; Liu X *et al.* 2022). ROS, as secondary messengers, further activate MAPK cascades and antioxidant defenses, including the glutathione metabolism pathway involving GPX, GST, and GSR, which help neutralize excess ROS generated by stress and maintain cellular homeostasis. These changes help eliminate excess ROS generated during mechanical stress, thereby enhancing cellular adaptability under stress conditions, and may also influence the development of tea quality (Li *et al.* 2020; Zhang *et al.* 2020; Dorion *et al.* 2021; Ni *et al.* 2021; Xue *et al.* 2023). Our transcriptomic and proteomic data also demonstrated that mechanical stress induced the upregulation of *CDPKs*, *Rbohs*, *CaCMLs*, and their corresponding proteins, indicating that tea leaves mount a typical abiotic stress response network in response to shaking. Importantly, these Ca^{2+}- and ROS-mediated pathways interface with hormonal signaling, particularly the JA signaling pathway. As a core regulator of mechanical stress responses, JA modulates defense and secondary metabolic pathways in various plant species. JA, JA-Ile, and MeJA enhance secondary metabolism by regulating genes such as *JAZ* and *CsAP2* (Zheng *et al.* 2020; Zhu *et al.* 2023). Specifically, during tea processing, JA-Ile accumulates during the shaking stage, enhancing key volatile biosynthesis through transcriptional regulation, whereas MeJA reshapes volatile profiles and reduces aromatic amino acids to fine-tune aroma composition (Shi *et al.* 2019; Zhu *et al.* 2019). In our study, genes and proteins associated with JA signaling were upregulated — *JAZ* showed significant increases, and *MYC2*, its downstream target, was partially upregulated — demonstrating activation of the JA signaling cascade. These results confirm that JA plays a central regulatory role in the mechanical stress response of tea leaves.

Environmental stresses such as mechanical wounding also activate quality-related metabolic pathways that produce volatile compounds primarily derived from fatty acids, terpenoids, and phenylpropanoids (Song *et al.* 2018; Zeng *et al.* 2018; Zhao *et al.* 2020; Li *et al.* 2023). Mechanical stress

during postharvest processing has been shown to upregulate LOX expression and activate the α-linolenic acid pathway, largely mediated by the activities of LOX and ADH, resulting in increased jasmine lactone — a key floral volatile in oolong tea (Hu *et al.* 2020; Zhou *et al.* 2021; Liu S *et al.* 2022). In this study, mechanical stress activated the α-linolenic acid metabolism pathway, as evidenced by enhanced *LOX* gene and protein expression. Simultaneously, *ADH1* downregulation may have limited the conversion of 3-hexenal to 3-hexenol, potentially accounting for the prominent grassy aroma observed in the early stages of shaking. Phenylalanine, a precursor for the biosynthesis of flavonoids and aromatic compounds such as phenylacetaldehyde, phenylacetic acid, and 2-phenylethanol, also plays a central role (Kaminaga *et al.* 2006; Sakai *et al.* 2007). Studies in roses have shown that mechanical stress enhances phenylalanine conversion to 2-phenylethanol through upregulation of biosynthetic enzymes such as ARO and PAR (Yang *et al.* 2009). In our findings, *PASS*, *PAR*, *ARO*, and *ADHs* genes and ARO, ADHs proteins were upregulated in phenylalanine metabolism under mechanical stress. Moreover, metabolomic data indicated that mechanical stress significantly increased the accumulation of cinnamic acid, 2-phenylethanol, and benzyl alcohol in agreement with previous studies showing that phenylpropanoid-derived volatiles accumulate under abiotic stress conditions (Kumar *et al.* 2013; Li *et al.* 2023). This suggests that mechanical stress activates phenylalanine-derived pathways, promoting the biosynthesis of aroma-related precursors that contribute to the distinctive fragrance of oolong tea.

5. Conclusion

This study demonstrates that mechanical stress promotes the development of tea quality by inducing the accumulation of key secondary metabolites through a hierarchical regulatory network that integrates DAMPs-triggered signaling cascades — such as Ca^{2+} influx, ROS generation, and phytohormones signaling — with multi-omics-driven metabolic reprogramming. The finding reveal that phenylalanine-derived volatiles (e.g., 2-phenylethanol, benzyl alcohol) and α-linolenic acid-derived jasmine lactone jointly contribute to the accumulation of characteristic aroma compounds in oolong tea. The transcriptional and translational activation of *LOX* and *PAR* genes, along with their encoded proteins, serves as a central regulatory switch in this process. Importantly, this work establishes a mechanistic framework linking the application of mechanical stress during tea processing to the biosynthesis of key flavor metabolites — bridging traditional empirical practices with molecular-level insights.

Acknowledgements

This study was supported by the National Key Research and Development Program of China (2022YFD2101101), the Earmarked Fund for CARS-19, the National Natural Science Foundation of China (32402634), the Modern Agricultural (Tea) Industry Technology System of Fujian Province, China (2025 No. 593) and the Special Fund for Science and Technology Innovation of Fujian Zhang Tianfu Tea Development Foundation, China (FJZTF01).

Declaration of competing interest

The authors declare that they have no conflict of interest.

Declaration of generative AI and AI-assisted technologies in the writing process

The authors declare that they did not use AI in the preparation and writing of this manuscript.

Appendices associated with this study are available at https://doi.org/10.1016/j.jia.2025.09.014

References

Beck J J, Smith L, Baig N. 2014. An overview of plant volatile metabolomics, sample treatment and reporting considerations with emphasis on mechanical damage and biological control of weeds. *Phytochemical Analysis*, **25**, 331–341.

Cai J, Aharoni A. 2022. Amino acids and their derivatives mediating defense priming and growth tradeoff. *Current Opinion in Plant Biology*, **69**, 102288.

Cao H, Li J, Ye Y, Lin H, Hao Z, Ye N, Yue C. 2020. Integrative transcriptomic and metabolic analyses provide insights into the role of trichomes in tea plant (*Camellia sinensis*). *Biomolecules*, **10**, 311.

Chen M, Zhang Y, Wang Y, Cheng P, Zhang Q, Li M, Jia X, Pan Y, Lin S, Luo Z, Wang H, Ye J. 2024. Transcriptomic analysis of the effect of shaking and tumbling degree on quality formation of wuyi rock tea. *Journal of Food Science*, **89**, 81–95.

Choi H W, Klessig D F. 2016. DAMPs, MAMPs, and NAMPs in plant innate immunity. *BMC Plant Biology*, **16**, 232.

Dorion S, Ouellet J C, Rivoal J. 2021. Glutathione metabolism in plants under stress: Beyond reactive oxygen species detoxification. *Metabolites*, **11**, 641.

Grabherr M G, Haas B J, Yassour M, Levin J Z, Thompson D A, Amit I, Adiconis X, Fan L, Raychowdhury R, Zeng Q, Chen Z, Mauceli E, Hacohen N, Gnirke A, Rhind N, Di Palma F, Birren B W, Nusbaum C, Lindblad-Toh K, Regev, A. 2011. Full-length transcriptome assembly from RNA-seq data without a reference genome. *Nature Biotechnology*, **29**, 644–652.

Guo X, Schwab W, Ho C T, Song C, Wan X. 2022. Characterization of the aroma profiles of oolong tea made from three tea cultivars by both GC-MS and GC-IMS. *Food Chemistry*, **376**, 131933.

Hao X, Horvath D, Chao W, Yang Y, Wang X, Xiao B. 2014. Identification and evaluation of reliable reference genes for quantitative real-time PCR analysis in tea plant (*Camellia sinensis* (L.) O. Kuntze). *International Journal of Molecular Sciences*, **15**, 22155–22172.

He H F, Wei K, Yin J, Ye Y. 2021. Insight into tea flavonoids: Composition and chemistry. *Food Reviews International*, **37**, 812–823.

Hou S, Liu D, He P. 2021. Phytocytokines function as immunological modulators of plant immunity. *Stress Biology*, **1**, 8.

Hu S, Chen Q, Guo F, Wang M, Zhao H, Wang Y, Ni D, Wang P. 2020. (*Z*)-3-hexen-1-ol accumulation enhances hyperosmotic stress tolerance in *Camellia sinensis*. *Plant Molecular Biology*, **103**, 287–302.

Huang X, Cao H, Guo Y, Liu J, Sun Y, Liu S, Lin J, Wei S, Wu L. 2020. The dynamic change of oolong tea constitutes during enzymatic-catalysed process of manufacturing. *International Journal of Food Science and Technology*, **55**, 3604–3612.

Huber A E, Bauerle T L. 2016. Long-distance plant signaling pathways in response to multiple stressors: The gap in knowledge. *Journal of Experimental Botany*, **67**, 2063–2079.

Kaminaga Y, Schnepp J, Peel G, Kish C M, Ben-Nissan G, Weiss D, Orlova I, Lavie O, Rhodes D, Wood K, Porterfield D M, Cooper A J L, Schloss J V, Pichersky E, Vainstein A, Dudareva N. 2006. Plant phenylacetaldehyde synthase is a bifunctional homotetrameric enzyme that catalyzes phenylalanine decarboxylation and oxidation. *Journal of Biological Chemistry*, **281**, 23357–23366.

Kumar S, Pandey A K. 2013. Chemistry and biological activities of flavonoids: An overview. *Scientific World Journal*, **2013**, 162750.

Li B, Dewey C N. 2011. RSEM: Accurate transcript quantification from RNA-seq data with or without a reference genome. *BMC Bioinformatics*, **12**, 323.

Li C, Lin J, Hu Q, Sun Y, Wu L. 2023. An integrated metabolomic

and transcriptomic analysis reveals the dynamic changes of key metabolites and flavor formation over tieguanyin oolong tea production. *Food Chemistry*: *X*, **20**, 100952.

Li H, Liu J X, Wang Y, Zhuang J. 2020. The ascorbate peroxidase 1 regulates ascorbic acid metabolism in fresh-cut leaves of tea plant during postharvest storage under light/dark conditions. *Plant Science*, **296**, 110500.

Lin J, Lin H, Li C, Liao N, Zheng Y, Yu X, Sun Y, Wu L. 2024. Unveiling characteristic metabolic accumulation over enzymatic-catalyzed process of tieguanyin oolong tea manufacturing by DESI-MSI and multiple-omics. *Food Research International*, **181**, 114136.

Lin J, Tu Z, Zhu H, Chen L, Wang Y, Yang Y, Lv H, Zhu Y, Yu L, Ye Y. 2022. Effects of shaking and withering processes on the aroma qualities of black tea. *Horticulturae*, **8**, 549.

Liu S, Guo L, Zhou Q, Jiang Z, Jin L, Zhu J, Xie H, Wei C. 2022. Identification and functional analysis of two alcohol dehydrogenase genes involved in catalyzing the reduction of (*Z*)-3-hexenal into (*Z*)-3-hexenol in tea plants (*Camellia sinensis*). *Journal of Agricultural and Food Chemistry*, **70**, 1830–1839.

Liu X, Zhao M, Gu C, Jiang H, Sun J, Li J. 2022. Genome-wide identification of MAPK family genes and their response to abiotic stresses in tea plant (*Camellia sinensis*). *Open Life Sciences*, **17**, 1064–1074.

Love M I, Huber W, Anders S. 2014. Moderated estimation of fold change and dispersion for RNA-seq data with DESeq2. *Genome Biology*, **15**, 550.

Meena M K, Prajapati R, Krishna D, Divakaran K, Pandey Y, Reichelt M, Mathew M K, Boland W, Mithöfer A, Vadassery J. 2019. The Ca^{2+} channel CNGC19 regulates arabidopsis defense against spodoptera herbivory. *The Plant Cell*, **31**, 1539–1562.

Ni T, Xu S, Wei Y, Li T, Jin G, Deng W W, Ning J. 2021. Understanding the promotion of withering treatment on quality of postharvest tea leaves using UHPLC-orbitrap-MS metabolomics integrated with TMT-based proteomics. *LWT-Food Science & Technology*, **147**, 111614.

O'Connell R J, Thon M R, Hacquard S, Amyotte S G, Kleemann J, Torres M F, Damm U, Buiate E A, Epstein L, Alkan N, Altmüller J, Alvarado-Balderrama L, Bauser C A, Becker C, Birren B W, Chen Z, Choi J, Crouch J A, Duvick J P, *et al.* 2012. Lifestyle transitions in plant pathogenic Colletotrichum fungi deciphered by genome and transcriptome analyses. *Nature Genetics*, **44**, 1060–1065.

Ruan J, Zhou Y, Zhou M, Yan J, Khurshid M, Weng W, Cheng J, Zhang K. 2019. Jasmonic acid signaling pathway in plants. *International Journal of Molecular Sciences*, **20**, 2479.

Sakai M, Hirata H, Sayama H, Sekiguchi K, Itano H, Asai T, Dohra H, Hara M, Watanabe N. 2007. Production of 2-phenylethanol in roses as the dominant floral scent compound fromL-phenylalanine by two key enzymes, a PLP-dependent decarboxylase and a phenylacetaldehyde reductase. *Bioscience*, *Biotechnology*, *and Biochemistry*, **71**, 2408–2419.

Shi J, Ma C, Qi D, Lv H, Yang T, Peng Q, Chen Z, Lin Z. 2015. Transcriptional responses and flavor volatiles biosynthesis in methyl jasmonate-treated tea leaves. *BMC Plant Biology*, **15**, 233.

Shi J, Xie D, Qi D, Peng Q, Chen Z, Schreiner M, Lin Z, Baldermann S. 2019. Methyl jasmonate-induced changes of flavor profiles during the processing of green, oolong, and black tea. *Frontiers in Plant Science*, **10**, 781.

Song C, Härtl K, McGrapher K, Hoffman T, Schwab W. 2018. Attractive but toxic: Emerging roles of glycosidically bound volatiles and glycosyltransferases involved in their formation. *Molecular Plant*, **11**, 1225–1236.

Wang D, Yoshimura T, Kubota K, Kobayashi A. 2000. Analysis of glycosidically bound aroma precursors in tea leaves. 1. Qualitative and quantitative analyses of glycosides with aglycons as aroma compounds. *Journal of Agricultural and Food Chemistry*, **48**, 5411–5418.

Wei C, Yang H, Wang S, Zhao J, Liu C, Gao L, Xia E, Lu Y, Tai Y, She G, Sun J, Cao H, Tong W, Gao Q, Li Y, Deng W, Jiang X, Wang W, Chen Q, Zhang S, *et al*. 2018. Draft genome sequence of Camellia sinensis var. sinensis provides insights into the evolution of the tea genome and tea quality. *Proceedings of the National Academy of Sciences of the United States of America*, **115**, E4151–E4158.

Wu L, Wang Y, Liu S, Sun Y, Li C, Lin J, Wei S. 2022. The stress-induced metabolites changes in the flavor formation of oolong tea during enzymatic-catalyzed process: A case study of zhangping shuixian tea. *Food Chemistry*, **391**, 133192.

Xue Z, Chen Z, Wang Y, Sun W. 2023. Proteomic analysis reveals the association between the pathways of glutathione and *α*-Linolenic acid metabolism and lanthanum accumulation in tea plants. *Molecules*, **28**, 1124.

Yang Z, Sakai M, Sayama H, Shimeno T, Yamaguchi K, Watanabe N. 2009. Elucidation of the biochemical pathway of 2-phenylethanol from shikimic acid using isolated protoplasts of rose flowers. *Journal of Plant Physiology*, **166**, 887–891.

Zeng L, Wang X, Xiao Y, Gu D, Liao Y, Xu X, Jia Y, Deng R, Song C, Yang Z. 2019a. Elucidation of (*Z*)-3-hexenyl-*β*-glucopyranoside enhancement mechanism under stresses from the oolong tea manufacturing process. *Journal of Agricultural and Food Chemistry*, **67**, 6541–6550.

Zeng L, Watanabe N, Yang Z. 2019b. Understanding the biosyntheses and stress response mechanisms of aroma compounds in tea (*Camellia sinensis*) to safely and effectively improve tea aroma. *Critical Reviews in Food Science and Nutrition*, **59**, 2321–2334.

Zeng L, Zhou Y, Fu X, Liao Y, Yuan Y, Jia Y, Dong F, Yang Z. 2018. Biosynthesis of jasmine lactone in tea (C*amellia sinensis*) leaves and its formation in response to multiple stresses. *Journal of Agricultural and Food Chemistry*, **66**, 3899–3909.

Zhang G, Yang J, Cui D, Zhao D, Li Y, Wan X, Zhao J. 2020. Transcriptome and metabolic profiling unveiled roles of peroxidases in theaflavin production in black tea processing and determination of tea processing suitability. *Journal of Agricultural and Food Chemistry*, **68**, 3528–3538.

Zhang H, Zhu J, Gong Z, Zhu J K. 2022. Abiotic stress responses in plants. *Nature Reviews Genetics*, **23**, 104–119.

Zhang N, Jing T, Zhao M, Jin J, Xu M, Chen Y, Zhang S, Wan X, Schwab W, Song C. 2019. Untargeted metabolomics coupled with chemometrics analysis reveals potential non-volatile markers during oolong tea shaking. *Food Research International*, **123**, 125–134.

Zhang X, Yu Y, Zhang J, Qian X, Li X, Sun X. 2024. Recent progress regarding jasmonates in tea plants: Biosynthesis, signaling, and function in stress responses. *International Journal of Molecular Sciences*, **25**, 1079.

Zhao M, Zhang N, Gao T, Jin J, Jing T, Wang J, Wu Y, Wan X, Schwab W, Song C. 2020. Sesquiterpene glucosylation mediated by glucosyltransferase UGT91Q2 is involved in the modulation of cold stress tolerance in tea plants. *New Phytologist*, **226**, 362–372.

Zheng Y, Chen X, Wang P, Sun Y, Yue C, Ye N. 2020. Genome-wide and expression pattern analysis of *JAZ* family involved in stress responses and postharvest processing treatments in *Camellia sinensis*. *Scientific Reports*, **10**, 2792.

Zhou Z, Wu Q, Ni Z, Hu Q, Yang Y, Zheng Y, Bi W, Deng H, Liu Z, Ye N, Lai Z, Sun Y. 2021. Metabolic flow of C6 volatile compounds from LOX-HPL pathway based on airflow during the post-harvest process of oolong tea. *Frontiers in Plant Science*, **12**, 738445.

Zhou Z, Wu Q, Rao H, Cai L, Zheng S, Sun Y. 2023. The dynamic change in aromatic compounds and their relationship with *CsAAAT* genes during the post-harvest process of oolong tea. *Metabolites*, **13**, 868.

Zhu C, Zhang S, Fu H, Zhou C, Chen L, Li X, Lin Y, Lai Z, Guo Y. 2019. Transcriptome and phytochemical analyses provide new insights into long non-coding RNAs modulating characteristic secondary metabolites of oolong tea (*Camellia sinensis*) in solar-withering. *Frontiers in Plant Science*, **10**, 1638.

Zhu Q, Liu L, Lu X, Du X, Xiang P, Cheng B, Tan M, Huang J, Wu L, Kong W, Shi Y, Wu L, Lin J. 2023. The biosynthesis of EGCG, theanine and caffeine in response to temperature is mediated by hormone signal transduction factors in tea plant (*Camellia sinensis L.*). *Frontiers in Plant Science*, **14**, 1149182.

Executive Editor-in-Chief Qiang Wang
Managing Editor Han Zhang